Miner Deposita (2016) 51:237–248
DOI 10.1007/s00126-015-0606-z

ARTICLE

Re–Os and U–Pb geochronology of the Laochang Pb–Zn–Ag and concealed porphyry Mo mineralization along the Changning–Menglian suture, SW China: implications for ore genesis and porphyry Cu–Mo exploration

Xiao-Dong Deng[1,2] **· Jian-Wei Li**[1,2] **· Xin-Fu Zhao**[1] **· Hong-Qiang Wang**[2] **· Liang Qi**[3]

Received: 18 February 2015 / Accepted: 13 July 2015 / Published online: 4 August 2015

Abstract Numerous polymetallic volcanogenic massive sulfide (VMS), vein, and replacement deposits are distributed along the Changning–Menglian suture zone in Sanjiang Tethyan metallogenic province, SW China. Laochang is the largest Pb–Zn–Ag vein and replacement deposit in this area, with a proven reserve of 0.51 Mt Pb, 0.34 Mt Zn, and 1,737 t Ag. Its age and relationship to magmatic events and VMS deposits in the region, however, have long been debated. In this paper, we present pyrite Re–Os and titanite U–Pb ages aiming to provide significant insights into the timing and genesis of the Pb–Zn–Ag mineralization. Pyrite grains in textural equilibrium with galena, sphalerite, and chalcopyrite from stratabound Pb–Zn–Ag and Cu-bearing Pb–Zn–Ag orebodies have a Re–Os isochron age of 45.7±3.1 Ma (2σ, mean square weighted deviation (MSWD)=0.45), whereas titanite grains intergrown with sulfide minerals yield a weighted mean $^{206}Pb/^{238}U$ age of 43.4±1.2 Ma (2σ, n=8). A Mo-mineralized granitic porphyry intersected by recent drilling below the Laochang Pb–Zn–Ag ores yields a zircon U–Pb age of 44.4±0.4 Ma (2σ, n=12). Within analytical uncertainties, the ages of the Pb–Zn–Ag deposit and the concealed Mo-mineralized porphyry are indistinguishable, indicating that they are products of a single magmatic hydrothermal system. The results show that Laochang Pb–Zn–Ag deposit is significantly younger than the host mafic volcanic rock (zircon U–Pb age of 320.8±2.7 Ma; 2σ, n=12) and Silurian VMS deposits along the Changning–Menglian suture zone, arguing against its origin as a Carboniferous VMS deposit as many researchers claimed. The initial $^{187}Os/^{188}Os$ ratio (0.540±0.012) obtained from the pyrite Re–Os isochron suggests that metals were likely derived from the granitic porphyry that formed from a hybrid magma due to mixing of crustal- and mantle-derived melts, rather than from the mafic volcanic host rocks as previously thought. Our results favor that the Laochang Pb–Zn–Ag deposit is the shallow product of a porphyry Mo system. Thus, there is potential for discovery of porphyry Mo or Cu–Mo deposits below Laochang and similar Pb–Zn–Ag deposits in the Changning–Menglian suture zone.

Keywords Geochronology · Stratabound Pb–Zn–Ag mineralization · Porphyry Mo deposits · Changning–Menglian suture

Editorial handling: T. Bissig

Electronic supplementary material The online version of this article (doi:10.1007/s00126-015-0606-z) contains supplementary material, which is available to authorized users.

✉ Xiao-Dong Deng
dengxiaodong@cug.edu.cn

Jian-Wei Li
jwli@cug.edu.cn

[1] State Key Laboratory of Geological Processes and Mineral Resources, China University of Geosciences, Wuhan 430074, China

[2] Faculty of Earth Resources, China University of Geosciences, Wuhan 430074, China

[3] State Key Lab of Ore Deposit Geochemistry, Institute of Geochemistry, Chinese Academy of Sciences, Guiyang 550002, China

Introduction

The Sanjiang Tethyan metallogenic province (STMP) in the eastern Tibetan plateau is a well-endowed part of the giant eastern Tethyan metallogenic belt (Fig. 1a; Hou et al. 2007). Numerous porphyry Cu, Cu–Mo, and Cu–Au deposits define two sub-parallel porphyry belts in the STMP (Fig. 1a; Hou et al. 2006; Deng et al. 2014; Mao et al. 2014). These

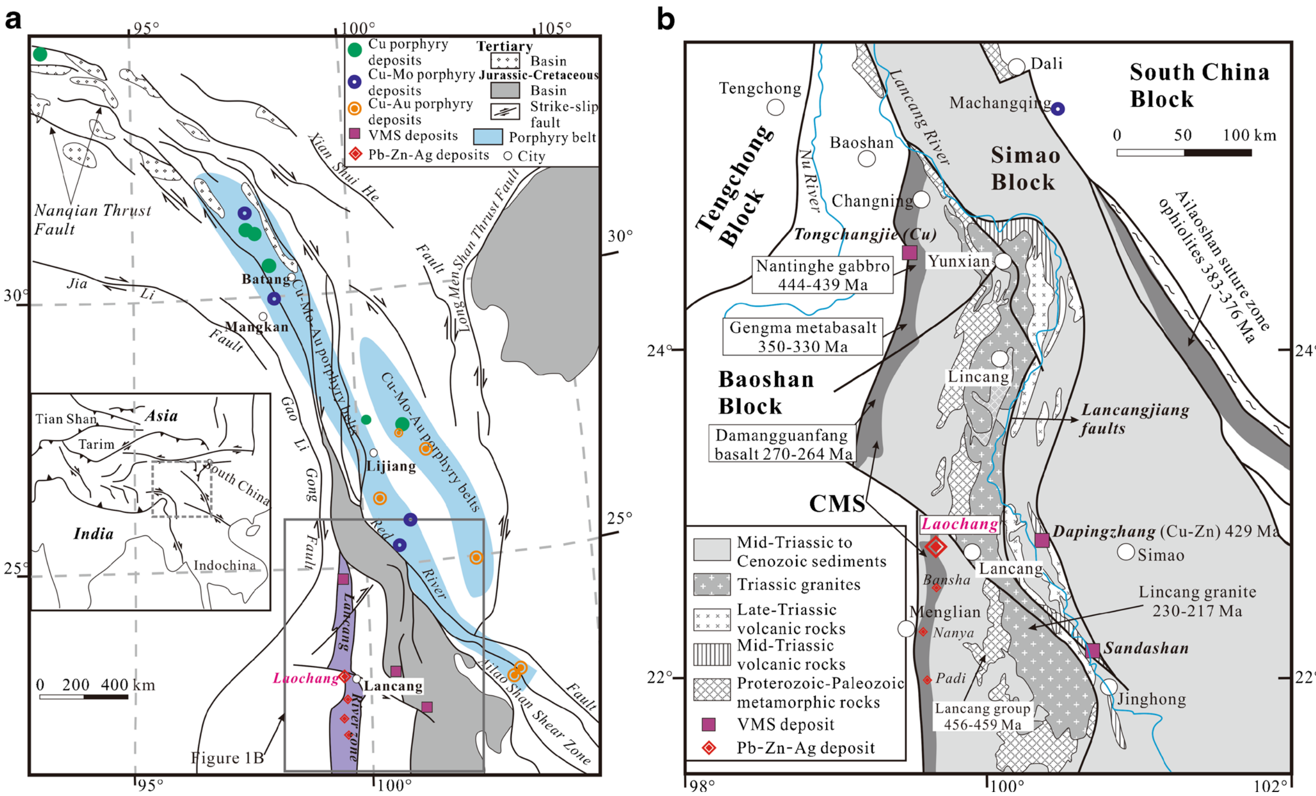

Fig. 1 Geologic map of the Sanjiang Tethyan metallogenic province (**a**) and Lancang river zone (**b**) showing the location of Laochang Pb–Zn–Ag deposit and other Eocene porphyry and Silurian VMS deposits. Geologic maps adapted from ECSGM (1986) and YBGMR (1990). Igneous rock ages are from Wang et al. (2013), Zhang and Duan (2001), Jian et al. (2009a), Nie et al. (2015), Hennig et al. (2009), Yang et al. (2014), and Lehmann et al. (2013)

porphyry deposits have molybdenite Re–Os ages ranging from 40.1±1.8 to 33.1±0.8 Ma, indicating that they are related to subduction of the Indian oceanic plate below Eurasia and subsequent India-Eurasia continental collision (Wang et al. 2005; Hou et al. 2006, 2007; Zeng et al. 2006; He et al. 2013, Deng et al. 2014). Southwest of the two porphyry zones, a number of Pb–Zn–Ag vein and replacement deposits are distributed along the Changning–Menglian suture (CMS) zone, but whether the Pb–Zn–Ag mineralization is genetically related to a porphyry Cu–Mo system is not clear and has been a prolonged debate, as porphyry Cu–Mo (Au) deposits are generally absent in this area (Fig. 1b).

Laochang Pb–Zn–Ag deposit in the CMS of southwestern STMP (Fig. 1a) has been mined since the fifteenth century (Yang and Mo 1993). Some researchers proposed that Laochang and other Pb–Zn–Ag deposits in this district are shallow manifestations of Eocene porphyry systems (Xue 1989; Wang 2007; Long et al. 2008; Li et al. 2010a). This interpretation is supported by recent deep drilling that has revealed Mo mineralization in concealed granitic porphyry. Others, in contrast, claimed that Laochang is a volcanogenic massive sulfide (VMS) deposit related to the Carboniferous volcanic rocks (Fan 1985; Yang and Mo 1993; Yang et al. 1999; Hou et al. 2007; Li et al. 2015). The host volcanic rocks at Laochang yielded a zircon U–Pb age of 324±3 Ma (Chen et al. 2010), which is significantly younger than Cu-dominated VMS deposits (e.g., Tongchangjie, 444–439 Ma; Fig. 1b; Wang et al. 2013) in northern CMS and Cu–Pb–Zn VMS deposits (e.g., Dapingzhang, 429±3 Ma; Lehmann et al. 2013) on the eastern side of this belt (Fig. 1b). The different models place Laochang into two different geologic settings: one related to Carboniferous mafic alkali volcanism in a continental rift setting and the other related to Eocene felsic plutonism in a continental collision setting.

In this paper, we present pyrite Re–Os and titanite U–Pb ages for the Laochang Pb–Zn–Ag deposit. In combination with zircon U–Pb ages of the host volcanic rocks and concealed Mo-mineralized granitic porphyry, these ages provide tight constraints on the timing of Pb–Zn–Ag mineralization and its relation to the host volcanic sequence and the hidden granitic porphyry. Our data provide convincing evidence that the Pb–Zn–Ag mineralization is the shallow product of a hidden porphyry Mo–(Cu) system. This finding has important implications for regional porphyry Mo and Cu–Mo deposit exploration.

Geological setting

The STMP in the eastern Tibetan plateau is composed of a mosaic of accreted terranes and blocks (Mo et al. 2001;

Burchfiel and Chen 2012; Metcalfe 2013). It has a complex history that reflects the opening and closure of the paleo-Tethys Ocean basin (Mo et al. 2001; Metcalfe 2013). The Lancang river zone in the southwest of STMP (Fig. 1a) is an amalgamation of four continental blocks (South China, Simao, Baoshan, and Tengchong blocks; Fig. 1b). The Simao block was separated from the South China block in Devonian (Zhong 1998; Jian et al. 2009a), whereas the Tengchong and Baoshan blocks were separated from the NE Gondwana in the early Permian (Metcalfe 2006). All these blocks were amalgamated in the Late Triassic during closure of the paleo-Tethys Ocean and intruded by the 300-km-long Lincang batholith (Fig. 1b; Metcalfe 2006; Hennig et al. 2009).

The Simao block is covered by Middle Triassic limestones and Cenozoic terrestrial sedimentary rocks and exhibits one magmatic zone (Yunxian-Jinghong) and two suture zones (Fig. 1b). The Yunxian–Jinghong magmatic zone is dominated by the north trending Lincang batholith (locally called Lincang granite), which is surrounded by metamorphosed volcanic rocks. The Lincang batholith is composed of monzonite, granite, and granodiorite (Heppe et al. 2007), which were emplaced between 230 and 217 Ma (Hennig et al. 2009; Yang et al. 2014). To the west of Lincang batholith, the Lancang Group is dominated by blue schist and amphibolite facies metamorphic rocks (Fig. 1b) consisting of meta-sandstones, sericite-quartz schists, chlorite schists, and amphibole-epidote-bearing metavolcanic rocks (Zhang et al. 1993). Previous Sm–Nd and Rb–Sr isochron ages on metavolcanic rocks in the Lancang Group were between 2.0 and 1.3 Ga (Zhai et al. 1990; Zhong 1998). Recent zircon U–Pb dating, however, indicates that volcanism occurred between 459 and 456 Ma (Nie et al. 2015). The $^{40}Ar/^{39}Ar$ and K–Ar ages show that the Lancang Group underwent metamorphism at 279–214 Ma (Zhang et al. 1993; Zhong et al. 2000; Heppe et al. 2007). To east of the Lincang batholith, the volcanic sequences are dominated by Permian mafic–ultramafic complexes and Triassic rhyolites and basalts (Fig. 1b), with minor Silurian rhyolite–dacite–andesite volcanics exposed in tectonic windows through the Middle Triassic to Cenozoic sedimentary sequence (Lehmann et al. 2013). The Silurian volcanics formed in a back-arc setting (Jian et al. 2009b; Lehmann et al. 2013).

The marginal areas of the Simao block are defined by two suture zones (Fig. 1b). The Ailaoshan suture zone on the eastern margin is marked by gabbro, anorthosite, and MORB, with zircon U–Pb ages of 383–376 Ma (Jian et al. 2009a). The CMS zone along the western margin is mainly composed of Paleozoic sedimentary and volcanic rocks (Fig. 1b). The sedimentary rocks include the Devonian cherts, sandstones and shales, and Late Carboniferous to Early Permian dolomites and dolomitic limestones. In the northern part of the CMS, volcanic rocks consist mainly of Early Silurian Nantinghe gabbro and meta-basalts (444–439 Ma; Wang et al. 2013), early Carboniferous Gengma meta-basalts (350–330 Ma; Zhang and Duan 2001), and Late Permian Damangguanfang basalts (270–264 Ma; Jian et al. 2009a). In the southern part of the CMS, volcanic rocks are dominated by the early Carboniferous Yiliu Group (Yang and Mo 1993), which has a zircon U–Pb age of 324±3 Ma (Chen et al. 2010). Several Pb–Zn–Ag deposits occur within the Yiliu Group (Fig. 1b).

Geology of the Laochang Pb–Zn–Ag deposit

The Laochang deposit (22° 45 N, 99° 44 E) is located about 30 km northwest of Lancang City (Fig. 1). It is the largest Pb–Zn–Ag deposit at the CMS and has a proven reserve of 1,737 t Ag (57.5–635 g/t), 0.51 Mt Pb (1.2–8.9 wt%), 0.34 Mt Zn (2.9–5.1 wt%), and 0.1 Mt Cu (0.1–0.8 wt%) (Li et al. 2010a). Below the Pb–Zn–Ag orebodies, there is a recently discovered porphyry and skarn Mo resource containing 117, 800 t Mo with a grade of 0.041–0.171 wt% (Li et al. 2010a). The Laochang deposit is hosted in early Carboniferous volcanic rocks (Yiliu Group) and Late Carboniferous to Early Permian marine carbonate rocks (Figs. 2 and 3). The early Carboniferous volcanic succession includes, from bottom to top (Fig. 2), (1) massive basalt to basaltic andesite and amygdaloidal andesite, 60–160-m thick; (2) andesitic pyroclastics with intercalated sandstone, shale, and limestone lenses, 0–20-m thick; (3) trachyandesitic lapilli and tuff with intercalated shale and limestone lenses, >22-m thick; (4) basaltic pyroclastics to massive flows, 55–160-m thick; and (5) tuffite and calcareous siltstone and limestone, 5–150-m thick (Yang and Mo 1993; Feng 2002). The volcanic sequence was conformably overlain by widespread Late Carboniferous to Early Permian limestones and dolomitic limestones (Fig. 2), with a total thickness of 570–900 m. The mining area and surroundings are variably mantled by colluvium or regolith. The volcanic rocks are fault-bounded by N- to NW-trending, steeply east dipping thrust faults (Fig. 2). Numerous secondary and higher order NE- or W-trending faults in carbonate rocks served to localize the Pb–Zn–Ag veins (Fig. 2).

Recent drill holes have encountered granitic porphyry at >300–900 m below the surface (Fig. 3; Li et al. 2010a). The porphyry is gray and contains phenocrysts of K-feldspar (10–15 vol%; up to 15-mm diameter), plagioclase (~10 % vol%; An=10–20; altered by sericite and carbonate), quartz (~10 vol%; rounded or embayed shape), and biotite (~5 vol%; replaced by chlorite, pyrite, and iron oxides). Groundmass is aplitic (10–200 μm) and composed of orthoclase and quartz. Geochemical data indicate that the felsic magma was produced by partial melting of mafic lower crust with input of minor amounts of mantle-derived melts (Yang et al. 2012). SHRIMP zircon U–Pb dating indicates that the porphyry was emplaced at 44.6±1.1 Ma (Li et al. 2010a).

Five types of sulfide mineralization are present in the Laochang deposit, which are, from top to bottom, vein Pb–

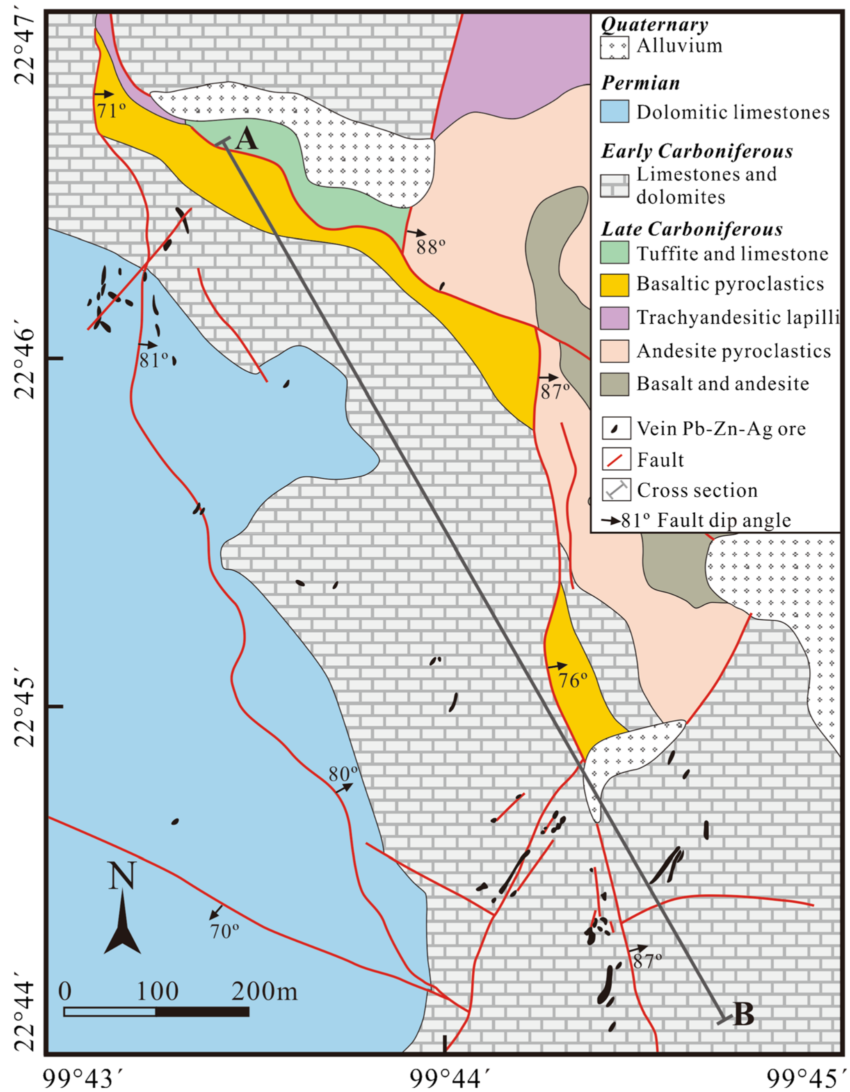

Fig. 2 Geologic map of the Laochang Pb–Zn–Ag deposit showing the distribution orebodies in Late Carboniferous to Permian carbonate rocks and the location of the cross section in Fig. 3 (after Li et al. 2010a

Zn–Ag (0–300 m below the surface), stratabound Pb–Zn–Ag (100–400 m), stratabound Cu-bearing Pb–Zn–Ag (400–700 m), skarn Mo (600–1,000 m), and porphyry Mo stockwork (>800 m) mineralization (Fig. 3; Li et al. 2010a). The Pb–Zn–Ag veins ranging from 0.3- to 15-m wide have the highest grades with 1.83–20.34 wt% Pb, 1.41–8.92 wt% Zn, and 96–635 g/t Ag. They mainly occur in Late Carboniferous to Early Permian marine carbonate and commonly follow stratigraphic intervals, fracture zones, and faults (Figs. 2 and 3). Hydrothermal alteration on both sides of individual Pb–Zn–Ag veins is dominated by calcite, ankerite, and rhodochrosite. These carbonate minerals commonly occur as fracture-infillings of a few millimeter to several centimeter width. Galena, sphalerite, and pyrite are the main sulfide phases, locally coexisting with minor amounts of chalcopyrite, aramayoite, and siderite. The stratabound Pb–Zn–Ag and Cu-bearing Pb–Zn–Ag orebodies are lenticular in shape, hosted in early Carboniferous volcanic rocks, and exhibit replacement textures. The stratabound Pb–Zn–Ag ores contain 0.88–10.16 wt% Pb, 0.85–4.97 wt% Zn, 59–217 g/t Ag, and 0.07–0.28 wt% Cu, whereas the Cu-bearing Pb–Zn–Ag ores have 0.18–5.26 wt% Pb, 0.40–2.18 wt% Zn, 20–167 g/t Ag, and 0.10–2.15 wt% Cu. The host volcanic rocks of stratabound Pb-Zn-Ag ores are intensely altered to epidote, chlorite, calcite, and clay (propylitic alteration), whereas those of Cu-bearing Pb–Zn–Ag ores are enveloped by sericite and quartz (phyllic alteration). Pyrite, Ag-bearing galena, and sphalerite are the main sulfide phases in stratabound Pb–Zn–Ag ores, with minor amounts of arsenopyrite, pyrrhotite, aramayoite, and native silver. The Cu-bearing Pb–Zn–Ag ores commonly consist of pyrite, galena, chalcopyrite, and sphalerite, with minor pyrrhotite, native silver, and scheelite.

Skarn Mo mineralization mainly occurs in the Early Carboniferous trachyandesite and basalt, whereas porphyry Mo mineralization is mainly distributed within granitic porphyry (Fig. 3). The skarn Mo orebodies are irregularly distributed along the contact zones between the Early Carboniferous trachyandesite and Eocene granitic porphyry (Fig. 3). The

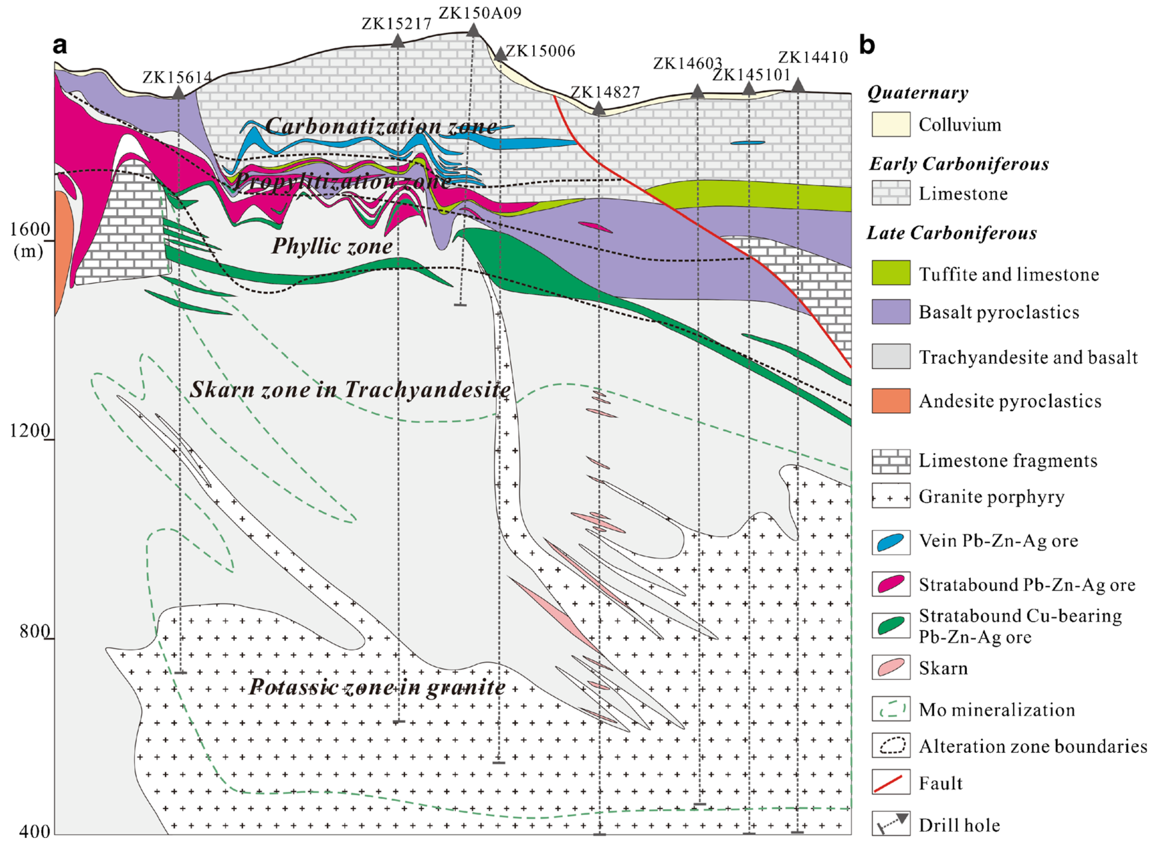

Fig. 3 Geologic cross section **a**, **b** showing the distribution of alteration and mineralization in the Laochang deposit (after Li et al. 2010a

skarn assemblages include prograde (e.g., diopside, garnet; Fig. 4a) and retrograde (e.g., epidote, actinolite, tremolite, chlorite, and vesuvianite) minerals. The main sulfide minerals include molybdenite, chalcopyrite, pyrite, and pyrrhotite, which are accompanied by minor amounts of oxide minerals such as scheelite and cassiterite. Porphyry Mo mineralization is characterized by quartz–sulfide veins, stockworks, and dense to sparse sulfide disseminations in altered granite, mostly at depths >800 m (Fig. 3). The ore-related alteration is dominated by K-feldspar, sericite, and quartz (Fig. 4b). Molybdenite is commonly intergrown with pyrite, chalcopyrite, and arsenopyrite.

Samples and analytical methods

The volcanic rock (Fig. 4c) and granitic porphyry samples (Fig. 4d) used for zircon U–Pb dating were collected from the mining tunnel at 1,700 m elevation and ZK14830 drill core at 631 m elevation, respectively. The stratabound Pb–Zn–Ag ore used for titanite separation was also collected from the mining tunnel at 1,700 m elevation. Zircon and titanite grains were separated using conventional heavy liquid and magnetic methods and then handpicked under a binocular microscope. Mineral gains were mounted in epoxy containers and then polished to expose the interior of the minerals. The back-scattered electron (BSE) and cathodoluminescence (CL) imaging is used to characterize the morphology and internal structure of these minerals, using a Quanta 450 FEG SEM equipped with a SDD Inca X-Max 50 and a MonoCL 4+ detector at the State Key Laboratory of Geological Processes and Mineral Resources (GPMR), China University of Geosciences, Wuhan.

Uranium–Th–Pb isotopes of zircon and titanite were analyzed using an Agilent 7500a ICP-MS apparatus equipped with a DUV 193 nm ArF-excimer laser (MicroLas, Germany) hosted at GPMR. Detailed analytical procedures and data reduction method follow those in Liu et al. (2010a, b) and are briefly summarized here. A spot size of 32 μm, a repetition rate of 5 Hz, and an energy density of 6 J/cm^2 were applied to all analyses. Argon was used as the make-up gas and mixed with helium as the carrier gas via a T-connector before entering the ICP. Nitrogen was added into the central gas flow (Ar + He) of the Ar plasma to decrease the detection limit and improve precision (Hu et al. 2008). Each analysis incorporated a background acquisition of 20–30 s (gas blank) followed by 50 s data acquisition. Zircon standard 91500 was used as a calibration standard for mass discrimination and U–Th–Pb isotope fractionation (Li et al. 2010b; Deng et al. 2015). Preferred U–Th–Pb isotopic ratios used for 91500 are from Wiedenbeck et al. (1995). The precision and accuracy of U–Th–Pb dating with this technique have been evaluated by

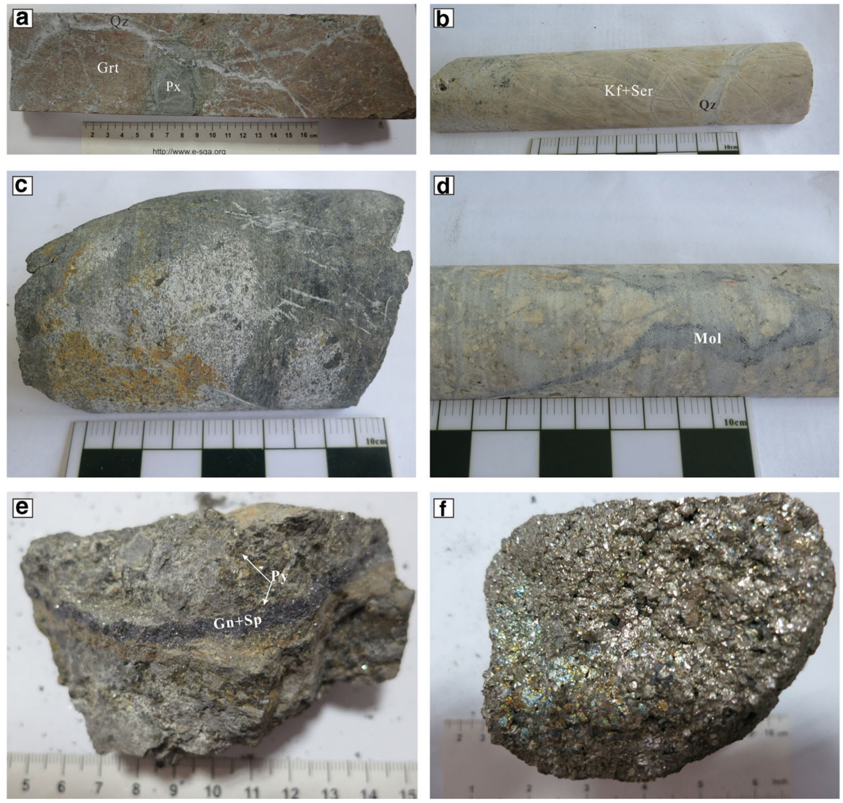

Fig. 4 Photographs of hydrothermal alteration and samples used for geochronological studies. **a** Skarn assemblages consisting of garnet and pyroxene are cut by quartz vein. **b** Potassic alteration consisting of K-feldspar, sericite, and quartz. **c** Phyllically altered mafic volcanic host rock. **d** Mo-mineralized granitic porphyry. **e** Stratabound Pb–Zn–Ag ore. **f** Stratabound Cu-bearing Pb–Zn–Ag ore. Mineral abbreviations: *Grt* garnet, *Px* pyroxene, *Qz* quartz, *Kf* K-feldspar, *Ser* sericite, *Mol* molybdenite, *Gn* galena, *Sp* sphalerite, *Py* pyrite

comparison with zircon standard GJ-1 (Jackson et al. 2004). Uranium and Th contents were calibrated against the glass standard NIST SRM610 combined with internal standardization (Si). Off-line selection and integration of background and analyzed signals and time-drift correction and quantitative calibration for U–Th–Pb dating were performed by ICPMSDataCal (Liu et al. 2010b). Uncertainties of preferred values for the external standard 91500 were propagated into the final results of the samples. Concordia diagrams and weighted mean calculations were plotted using Isoplot/Ex_ver3 (Ludwig 2003).

Stratabound Pb–Zn–Ag (Fig. 4e) and Cu-bearing Pb–Zn–Ag ores for pyrite separation (Fig. 4f) were collected from 1,700 and 1,600 m elevation tunnels, respectively. Detailed analytical procedures are described in Qi et al. (2010). Pure pyrite separates of 2 to 3 g were accurately weighed according to the analyzed Re concentrations and were digested in a 200-ml re-usable Carius tube using aqua regia with rhenium and osmium spikes at 200 °C for about 10 h (Qi et al. 2013). Osmium was separated from the matrix by distillation, and Re was separated from the remaining solutions using anion exchange resin. Rhenium contents were measured using a PR ELAN DRC-e ICP-MS, whereas Os isotopes were determined with a Bruker Auraro M90 ICP-MS due to the extremely low Os contents. Total blanks were 6.4±1.1 pg for Re and 2.0±0.4 pg for Os. Uncertainties in Re and Os mass spectrometer measurements, blank abundances, and spike calibrations were propagated into the final results.

Results

Zircon U–Pb age

Laser ablation ICP-MS titanite U–Pb dating results are summarized as Electronic Supplementary Material (ESM 1: Table S1). Zircon grains from Mo-mineralized granitic porphyry are colorless to pale brown and 50–350-μm long, with length/width ratios of 2–4. In CL images, most grains exhibit bright cores with oscillatory zoned rims, typical of magmatic zircon (Fig. 5a). Zircon crystals have high U (577–2,528 ppm) and Th (117–1,164 ppm) contents, with Th/U ratios of 0.1–0.5 (ESM 1: Table S1). Twelve spot analyses on ten zircon grains yield concordant $^{206}Pb/^{238}U$ ages ranging from 43±2 to 45±1 Ma (ESM 1: Table S1 and Fig. 5a), with a weighted mean of 44.4±0.4 Ma (2σ, mean square weighted deviation (MSWD)=1.3). Two spots from two zircon cores have relatively old $^{206}Pb/^{238}U$ ages of 214±5 and 229±6 Ma, which are interpreted to be inherited components.

Zircon grains from the host volcanic rock can be classified into three types. Type 1 zircon grains are subhedral to anhedral, >100-μm long, and exhibit irregular zoning in CL images. They have low U (182–

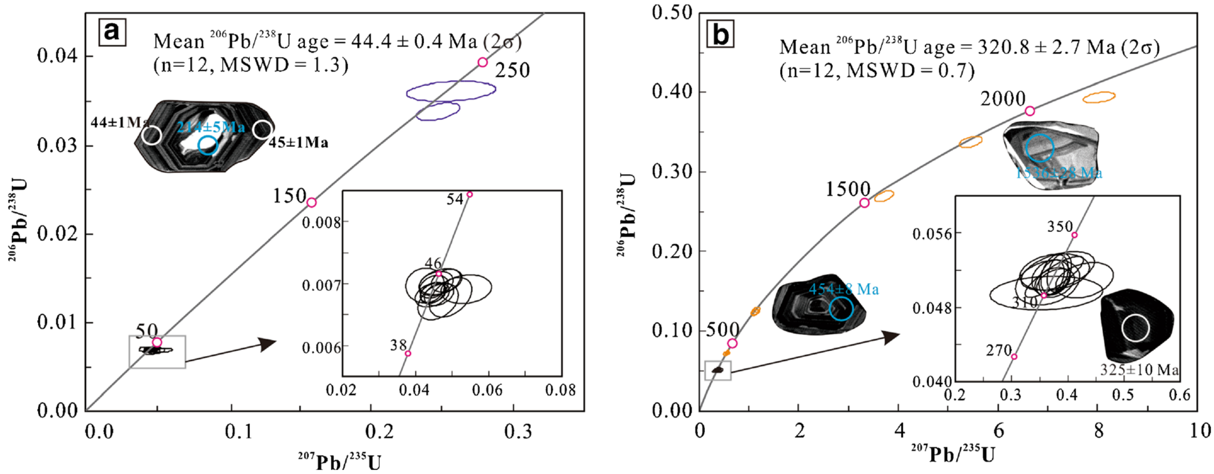

Fig. 5 CL images and U–Pb concordia diagrams for zircon grains in granitic porphyry (**a**) and the host volcanic rock (**b**) from the Laochang deposit

535 ppm) and Th (57–353 ppm) contents, with Th/U ratios of 0.2–1.0 (ESM 1: Table S1). Six spot analyses on type 1 zircon yield relatively old U–Pb ages, ranging from 765±31 to 2,234±29 Ma (ESM 1: Table S1 and Fig. 5b). Type 2 zircon grains are dark to brown, subhedral, 50–150-μm long, and display irregular zoning in CL images (Fig. 5b). They have variable U (183–1,112 ppm) and Th (52–483 ppm), with Th/U ratios of 0.3–0.8 (ESM 1: Table S1). Five analyses yield ^{206}Pb/^{238}U ages ranging from 445±10 to 455±14 Ma, with a weighted mean of 449±4 Ma (2σ, MSWD=0.8). Type 3 zircon grains are subhedral to euhedral, 30–100-μm long, and have wide zoning bands in CL images (Fig. 5b). Uranium and Th concentrations are high but relatively variable, ranging from 125 to 3,127 ppm and 190 to 8,249 ppm, respectively (ESM 1: Table S1), with Th/U ratios at 0.7–9.8. Twelve spots on type 3 zircon have ^{206}Pb/^{238}U ages ranging from 312±9 to 326±10 Ma (Fig. 5b), with a weighted mean age of 320.8±2.7 Ma (2σ, MSWD=0.7).

Titanite U–Pb age

Titanite grains extracted from stratabound Pb–Zn–Ag ore are subhedral and commonly intergrown with sulfide minerals and hydrothermal calcite (Fig. 6a). They have low but variable U (39–551 ppm) and Th (31–207 ppm), with Th/U ratios of 0.2–1.5 (ESM 1: Table S1 and Fig. 6b). Eight spot analyses on eight grains have reproducible ^{206}Pb/^{238}U ages that range from 41±7 to 45±2 Ma (Fig. 6b), with a weighted mean of 43.4±1.2 Ma (2σ, MSWD=0.8).

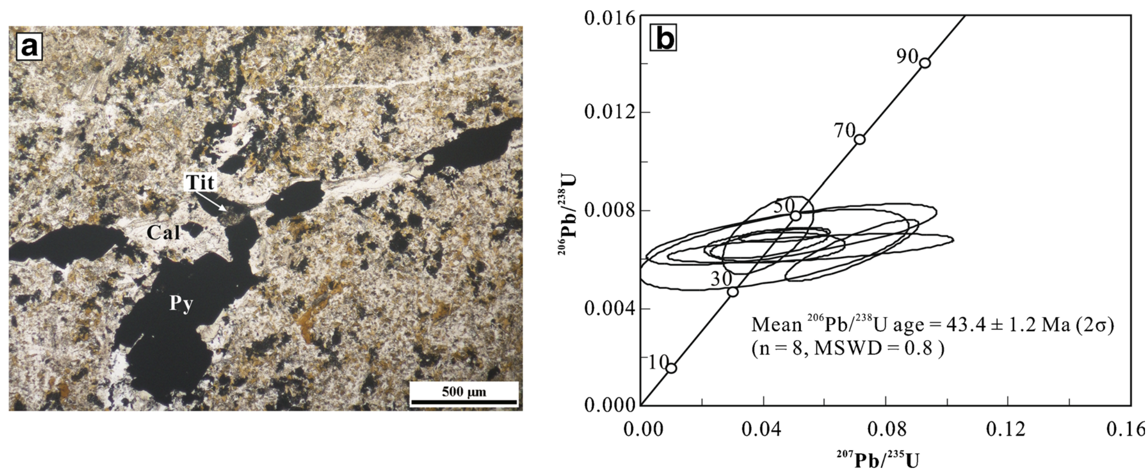

Fig. 6 **a** Photomicrograph of titanite grains intergrown with sulfide minerals and calcite in altered mafic volcanic rock from the Laochang Pb–Zn–Ag deposit. **b** U–Pb concordia diagram for titanite grains. Mineral abbreviations: *Tit* titanite, *Cal* calcite, *Py* pyrite

Pyrite Re–Os age

Pyrite grains from the stratabound Pb–Zn–Ag and Cu-bearing Pb–Zn–Ag ores are intergrown with sphalerite, galena, and chalcopyrite (Fig. 7a, b). All pyrite samples have relatively low total Re contents, ranging from 405 to 3,605 ppt with ^{187}Re abundance of 253 to 2,257 ppt (Table 1). The abundance of ^{187}Os in pyrite ranges from 0.72 to 4.41 ppt (Table 1). They contain high common Os ranging from 9.58 to 72.59 ppt and have $^{187}Re/^{188}Os$ ratios between 52 and 791. All six samples yield an isochron age of 45.7±3.1 Ma (MSWD=0.45) on the $^{187}Re/^{188}Os$ vs. $^{187}Os/^{188}Os$ plot, with an initial $^{187}Os/^{188}Os$ ratio of 0.540±0.012 (Fig. 7c).

Discussion

Age of the volcanic rocks hosting Laochang Pb–Zn–Ag deposit

The age of the volcanic rocks hosting Laochang Pb–Zn–Ag ores has been controversial (Yang and Mo 1993; Chen 1995; Feng 2002). Abundant bivalve-fauna and radiolarian assemblages have been found within chert and limestone fragments entrained in volcanic sequences at Laochang and have been interpreted to be late Permian in age (Feng and Liu 1993; Feng 2002). Previous whole-rock K–Ar dating on the volcanic rocks defined two age groups of 245–195 and 51–38 Ma (Chen 1995), suggesting the volcanic rocks may have formed in the Early Triassic and then were thermally overprinted by extensive Eocene magmatism along the Sanjiang Tethyan tectono-magmatic belts.

Our zircon U–Pb results on the volcanic rocks define three age groups. The oldest group has U–Pb ages from 2,234±29 to 765±31 Ma (Fig. 5b), which most likely reflect inherited components from the Precambrian basement underlying this area and widely distributed over the South China block (Zhou et al. 2002, 2014; Li et al. 2014). The intermediate group has U–Pb ages of 455–445 Ma (Fig. 5b) that are interpreted to be inherited from meta-basalts (444–439 Ma, Wang et al. 2013; Fig. 1b) and/or metavolcanic rocks of the early Silurian Lancang Group previously dated at 459–456 Ma (Nie et al. 2015; Fig. 1b), which underlies the district. The youngest group has a weighted mean $^{206}Pb/^{238}U$ age of 320.8±2.7 Ma (Fig. 5b), which we consider to be the best estimate for the eruption age of the host volcanic rocks. This view is confirmed by a SHRIMP zircon U–Pb age of 324±3 Ma (Chen et al. 2010) for volcanic tuff from the Laochang Pb–Zn–Ag deposit. Our new data are also consistent with U–Pb ages of meta-basalts in the Gengma area in the CMS (350–331 Ma; Zhang and Duan 2001; Fig. 1b). Together, our results demonstrated that the volcanic rocks hosting Pb–Zn–Ag mineralization at Laochang were erupted in the Early Carboniferous and

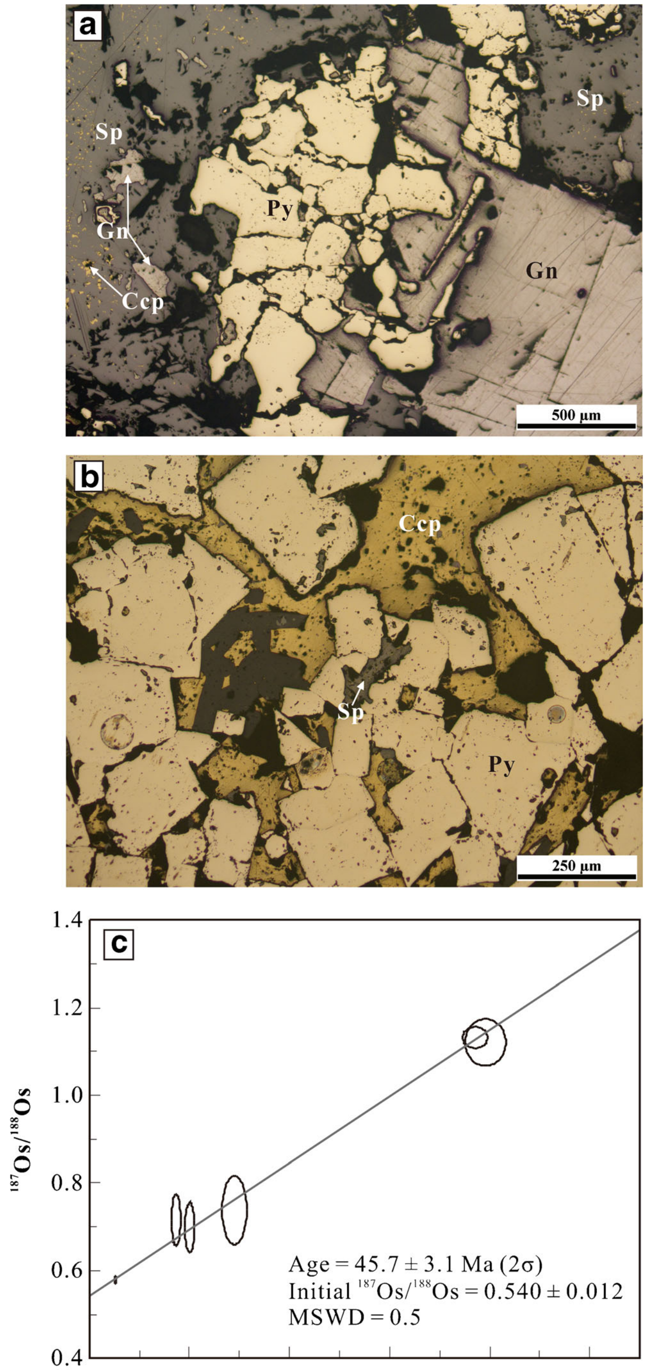

Fig. 7 Photomicrographs of stratabound Pb–Zn–Ag (**a**) and Cu-bearing Pb–Zn–Ag (**b**) ore samples from the Laochang deposit showing pyrite intergrown with galena, sphalerite, and chalcopyrite. **c** Re–Os isochron diagram for pyrite from ore samples. Mineral abbreviations: *Gn* galena, *Sp* sphalerite, *Ccp* chalcopyrite, *Py* pyrite

thus are products of coeval mafic-intermediate magmatism that are widely distributed along the CMS.

Our U–Pb zircon data indicate that the ages inferred from the paleontological stratigraphy are problematic and

Table 1 Re–Os isotope data for pyrite from the Laochang deposit

Sample	Re		^{187}Re		^{187}Os		Os_{com}		$^{187}Re/^{188}Os$		$^{187}Os/^{188}Os$	
	ppt	1σ	ppt	1σ	ppt	1σ	ppt	1σ		1σ		1σ
LC1700-01	590	15	369	9	0.77	0.04	9.58	0.48	290	16	0.738	0.052
LC1700-03	809	5	506	3	4.41	0.08	72.59	1.83	52	1	0.579	0.006
LC1700-05	482	6	302	4	1.02	0.04	13.10	0.41	173	6	0.716	0.039
LC1600-08	3,605	56	2,257	35	2.92	0.05	22.01	0.32	771	16	1.131	0.016
LC1600-09	2,872	65	1,798	41	2.25	0.02	17.09	0.44	791	27	1.121	0.035
LC1600-17	405	9	253	6	0.72	0.04	9.49	0.20	201	6	0.698	0.038

unreliable when interpreted as the formation age of the volcanic rocks. We suggest that the fossil-bearing Late Permian sedimentary rocks are extraneous in origin as partly indicated by the fact that they are in structural contact with the volcanic sequences along thrust faults (Fig. 3; Feng 2002; Li et al. 2010a; Lehmann et al. 2013). The Triassic K–Ar ages (245–195 Ma; Chen et al. 1995) are consistent with the 250 to 200 Ma high-T/low-P metamorphism of the Lancang Group (Zhang et al. 1993; Zhong et al. 2000; Heppe et al. 2007), whereas the Eocene K-Ar ages (51–38 Ma; Chen et al. 1995) are evidence of a paleothermal anomaly related to the hidden granitic porphyry (44.4±0.4 Ma; Fig. 5a). Collectively, the volcanic rocks hosting the Laochang Pb–Zn–Ag deposit formed in the early Carboniferous and then were subsequently disturbed in Triassic metamorphic and Eocene magmatic events.

Age of mineralization

The Laochang deposit is dominated by shallow stratabound Pb–Zn–Ag and deep stockwork Mo mineralization. Previous Pb–Pb model ages on the Pb–Zn–Ag orebodies define three age groups at 351–336 Ma (Fan 1985), 147–98 Ma (Xue 1989), and 87–66 Ma (Ouyang and Xu 1991) that do not agree with dates obtained by other methods and are, therefore, geologically meaningless. In contrast, the previous Rb–Sr isochron age of 45 ±4 Ma (Long et al. 2008) on sphalerite and pyrite from the Pb–Zn–Ag orebodies agrees with our Re–Os date on ore-related pyrite of 45.7±3.1 Ma (Fig. 7c) and U–Pb date on hydrothermal titanite of 43.4±1.2 Ma (Fig. 6b). The Eocene ages on the stratabound Pb–Zn–Ag ores are consistent with the zircon U–Pb emplacement age of the hidden granitic porphyry (44.4±0.4 Ma; Fig. 5a) and the Re–Os age of stockwork molybdenite veins within it (43.4±0.8 Ma; Li et al. 2010a). Together, these results confirm that the Pb–Zn–Ag mineralization at shallow levels was within error contemporaneous with porphyry Mo mineralization at deeper levels.

Implications for ore genesis and regional exploration

Genesis of the stratabound Pb–Zn–Ag and Cu-bearing Pb–Zn–Ag orebodies in volcanic rocks at Laochang has long been debated (Fan 1985; Xue 1989). Previous studies have proposed that the Laochang Pb–Zn–Ag deposit is of VMS origin formed coevally with the host volcanic rocks (Fan 1985; Yang and Mo 1993; Yang et al. 1999; Hou et al. 2006; Li et al. 2015). If this model is correct, one would expect that Cu-mineralized pipes and stringer zones, typical of VMS deposits, would be present below the Pb–Zn–Ag ores as is the case in the Tongchangjie and Dapingzhang VMS deposits in the Sanjiang Tethyan metallogenic province (Li et al. 2010a; Lehmann et al. 2013). Our new geochronological results, however, demonstrate that the Pb–Zn–Ag mineralization is not of VMS origin in association with the volcanic rocks in the mine. This view is partly confirmed by geochemical features of the Pb–Zn–Ag ores. The Pb/Zn ratios of the Laochang

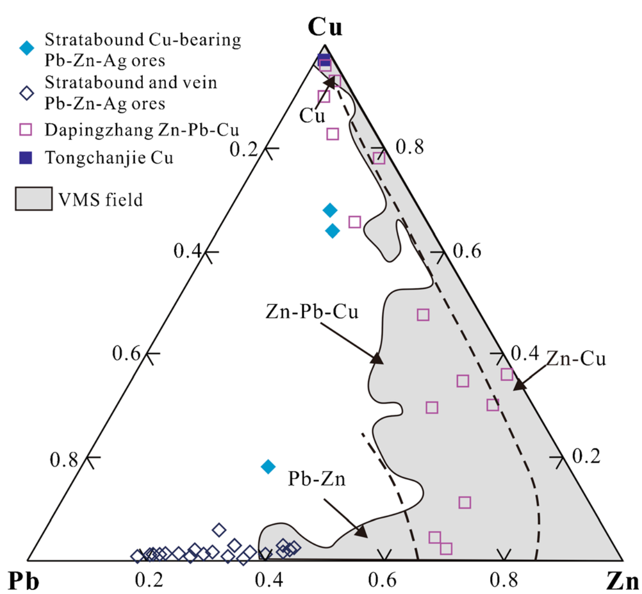

Fig. 8 Cu–Pb–Zn ternary diagram from Franklin (1996) that compares Laochang ore samples to those from the Dapingzhang and Tongchangjie VMS deposits

Pb–Zn–Ag ores (1.2–4.5; Li et al. 2010a) are significantly higher than those typically found in VMS deposits (Pb/Zn< 1; Franklin et al. 2005). In the Cu–Pb–Zn ternary diagram (Franklin 1996), samples from the Tongchangjie and Dapingzhang VMS deposits in the Sanjiang Tethyan metallogenic province plot within the VMS field, whereas samples from Laochang deviate this diagnostic area (Fig. 8).

Geological and geochronological data confirm that the Laochang Pb–Zn–Ag ores are genetically related to the hidden granitic porphyry with porphyry and skarn Mo mineralization. These ores are typically localized in permeable volcanic units, fractures, and/or Late Carboniferous to Permian carbonate rocks and exhibited conspicuous replacement textures (Figs. 2, 3, and 4). These features are consistent with polymetallic vein and replacement deposits associated with porphyry intrusions widely recognized in the world (e.g., Titley 1993; Plumlee et al. 1995; Mao et al. 2009, 2011). The lateral and vertical alteration patterns (Fig. 3; Li et al. 2010a), consisting predominantly of potassic (stockwork Mo mineralization), garnet–diopside (skarn Mo mineralization), phyllic (stratabound Cu–bearing Pb–Zn–Ag ores), propylitic (stratabound Pb–Zn–Ag ores), and Fe–Mn carbonatization (vein Pb–Zn–Ag ores), confirm that the Laochang hydrothermal system was initiated by a porphyry intrusion, as observed in other porphyry-epithermal systems (Simmons et al. 2005; Sillitoe 2010; Cooke et al. 2011).

The initial $^{187}Os/^{188}Os$ ratio (0.540±0.012) obtained from the pyrite Re–Os isochron (Fig. 5c) is between that of typical crustal (~1.0–1.5) and mantle (~0.12–0.13) sources (Shirey and Walker 1998) and thus indicating a hybrid igneous source for the ore fluids and other components in the fluids. The initial Os isotopic ratio of pyrite is consistent with previous geochemical studies demonstrating that the granitic porphyry formed by the mixing of mantle- and crustal-derived magmas (Xu and Ouyang 1991; Yang et al. 2012), but it is inconsistent with the mantle origin of the mafic volcanic rocks (Chen et al. 2011; Li et al. 2015). We therefore infer that metals and hydrothermal fluids were derived from granitic porphyry, rather than from mafic volcanic rocks. This interpretation is supported by the initial $^{87}Sr/^{86}Sr$ ratio obtained from the pyrite and sphalerite Rb–Sr isochron of 0.70977±0.00034 (Long et al. 2008), which is similar to the value of granitic porphyry (0.71127±0.00047; Ouyang and Xu 1991) but much higher than the early Carboniferous mafic volcanic rocks (0.70001; Long et al. 2008). In summary, the textural, geochemical, and isotopic evidence confirms that the Laochang Pb–Zn–Ag mineralization is spatially, temporally, and genetically related to the concealed Mo-mineralized porphyry.

Several other Pb–Zn–Ag deposits with propylitic and phyllic alteration halos similar to Laochang occur in early Carboniferous volcanic rocks along the CMS (Fig. 1b; Wang 2007). If they are related to concealed granitic porphyries, then the CMS may potentially become the third porphyry Cu–Mo–Au belt in the STMP (Fig. 1). This concept will have important implications for future exploration strategy in this giant metallogenic belt.

Conclusions

Pyrite intergrown with galena and sphalerite from the Laochang stratabound Pb–Zn–Ag and Cu-bearing Pb–Zn–Ag ores has a Re–Os isochron age of 45.7±3.1 Ma, whereas titanite grains coexisting with sulfide minerals from the stratabound Pb–Zn–Ag ores yield a weighted mean U–Pb age of 43.4±1.2 Ma. Both ages are consistent with a zircon U–Pb age (44.4±0.4 Ma) of a concealed Mo-mineralized granitic porphyry and a molybdenite Re–Os isochron age of 43.4 ±0.8 Ma on stockworks within this porphyry. The initial $^{187}Os/^{188}Os$ ratio of pyrite (0.540±0.012) allows that Os and, by inference, other melts in the hydrothermal ore fluids were sourced from the hidden granitic porphyry that formed by mixing of crustal and mantle-derived magmas revealed in previous studies. Meanwhile, the mafic volcanic rocks hosting the Pb–Zn–Ag mineralization have a zircon U–Pb age of 320.8±2.7 Ma, significantly older than the ores. Results from this study confirm that the Laochang stratabound and vein Pb–Zn–Ag ores are not parts of a Late Paleozoic VMS deposit as previously thought, rather they represent shallow expressions of a porphyry Mo system, both forming an important part of the giant Cenozoic Sanjiang Tethyan metallogenic province. We infer that similar Mo or Cu–Mo porphyry deposits may be present below other Pb–Zn–Ag deposits along the CMS that may be within reach of drilling.

Acknowledgments We thank Jianpei Lu, Suxin Zhang, Lu Wang, and Zhaochu Hu for their help during sample preparation, SEM, CL, and LA-ICP-MS analysis, respectively. We also thank Albert Hofstra at the USGS for his constructive review. Thomas Bissig, Jingwen Mao, and Bernd Lehmann provided detailed reviews and useful suggestions that helped improving presentation of the manuscript. This research was financially supported by the Natural Science Foundation of China (grants 41202053, 41325007), the International Postdoctoral Exchange Fellowship Program from China Postdoctoral Science Foundation, and the MOST special fund from the GPMR lab (MSFGPMR201304).

Compliance with ethical standards Our works do not contain conflicts of interest and human participants and/or animals. The submission adheres to the Publishing Ethics Policy of Springer.

References

Burchfiel BC, Chen Z (2012) Tectonics of the southeastern Tibetan Plateau and its adjacent foreland. Geological Society of America 210: 164 p.

Chen M, Huang Z, Luo T, Yan Z, Long H (2010) SHRIMP dating and its geological significance of zircon in volcanic from Laochang large

silver-lead-zinc deposit in Western Yunnan Province, China. Acta Mineralogica Sinica 30:456–462 (in Chinese with English abstract)
Chen M, Huang Z, Luo T, Yan Z, Long H (2011) Petrogenesis and tectonic significance of the Laochang basalt in western Yunnan province. Acta Geologica Sinica 31:55–61 (in Chinese with English abstract)
Chen Y (1995) Geological characteristics and genesis of Laochang volcanic-hosted silver, lead, zinc and copper deposit in Yunnan. Journal of Guilin Institute of Technology 15:124–130 (in Chinese with English abstract)
Cooke DR, Deyell CL, Waters PJ, Gonzales RI, Zaw K (2011) Evidence for magmatic-hydrothermal fluids and ore-forming processes in epithermal and porphyry deposits of the Baguio District, Philippines. Economic Geology 106:1399–1424
Deng J, Wang Q, Li G, Santosh M (2014) Cenozoic tectono-magmatic and metallogenic processes in the Sanjiang region, southwestern China. Earth-Science Reviews 138:268–299
Deng XD, Li JW, Zhou MF, Zhao XF, Yan DR (2015) In-situ LA-ICPMS trace elements and U–Pb analysis of titanite from the Mesozoic Ruanjiawan W–Cu–Mo skarn deposit, Daye district, China. Ore Geology Reviews 65:990–1004
ECSGM-Edit Committee of the Sangjiang Geological Map (1986) Geological map of the Jinshajiang, Langcangjiang, Nujiang regions. Beijing, Geological Publishing House, scale 1:1,000,000 (in Chinese).
Fan C (1985) Discussion on the origin and the regional geological background of Laochang Pb-Zn deposits in Lancang country. Yunnan Geology 4:1–16 (in Chinese with English abstract)
Feng QL (2002) Stratigraphy of volcanic rocks in the Changning-Menglian Belt in southwestern Yunnan, China. Journal of Asian Earth Sciences 20:657–664
Feng Q, Liu B (1993) Statigraphic investigation of the volcanic rocks in Changning-Menglian tectonic belt, southwestern Yunnan, China. Geoscience 7:402–409 (in Chinese with English abstract)
Franklin JM (1996) Volcanic-associated massive sulphide deposits. In: Eckstrand OR, Sinclair WD, Thorpe RI (eds) Geology of Canadian mineral deposit types, vol 8, Geology of Canada., pp 158–183
Franklin JM, Gibson HL, JonassonIR, Galley AG (2005) Volcanogenic massive sulfide deposits. Economic Geology 100th Anniversary Volume: 523–560.
He W, Mo X, Yu X, He Z, Dong G, Liu X, Su G, Huang X (2013) Zircon U-Pb and molybdenite Re-Os dating for the Beiya gold-polymetallic deposit in the western Yunnan Province and its geological significance. Acta Petrologica Sinica 29:1301–1310 (in Chinese with English abstract)
Hennig D, Lehmann B, Frei D, Belyatsky B, Zhao XF, Cabral AR, Zeng PS, Zhou MF, Schmidt K (2009) Early Permian seafloor to continental arc magmatism in the eastern Paleo-Tethys: U-Pb age and Nd-Sr isotope data from the southern Lancangjiang zone, Yunnan, China. Lithos 113:408–422
Heppe K, Helmcke D, Wemmer K (2007) The Lancang River Zone of southwestern Yunnan, China: a questionable location for the active continental margin of Paleotethys. Journal of Asian Earth Sciences 30:706–720
Hou Z, Zaw K, Pan G, Mo X, Xu Q, Hu Y, Li X (2007) Sanjiang Tethyan metallogenesis in SW China: tectonic setting, metallogenic epochs and deposit types. Ore Geology Reviews 31:48–87
Hou Z, Zeng P, Gao Y, Du A, Fu D (2006) Himalayan Cu-Mo-Au mineralization in the eastern Indo-Asian collision zone: constraints from Re-Os dating of molybdenite. Mineralium Deposita 41:22–45
Hu Z, Gao S, Liu Y, Hu S, Chen H, Yuan H (2008) Signal enhancement in laser ablation ICP-MS by addition of nitrogen in the central channel gas. Journal of Analytical Atomic Spectrometry 23:1093–1101
Jackson SE, Pearson NJ, Griffin WL, Belousova EA (2004) The application of laser ablation-inductively coupled plasma-mass spectrometry to in situ U-Pb zircon geochronology. Chemical Geology 211:47–69
Jian P, Liu D, Kröner A, Zhang Q, Wang Y, Sun X, Zhang W (2009a) Devonian to Permian plate tectonic cycle of the Paleo-Tethys Orogen in southwest China (II): insights from zircon ages of ophiolites, arc/back-arc assemblages and within-plate igneous rocks and generation of the Emeishan CFB province. Lithos 113:767–784
Jian P, Liu D, Krönerr A, Zhang Q, Wang Y, Sun X, Zhang W (2009b) Devonian to Permian plate tectonic cycle of the Paleo-Tethys Orogen in southwest China (I): geochemistry of ophiolites, arc/back-arc assemblages and within-plate igneous rocks. Lithos 113: 748–766
Lehmann B, Zhao X, Zhou M, Du A, Mao J, Zeng P, Henjes-Kunst F, Heppe K (2013) Mid-Silurian back-arc spreading at the northeastern margin of Gondwana: the Dapingzhang dacite-hosted massive sulfide deposit, Lancangjiang zone, southwestern Yunnan, China. Gondwana Research 24:648–663
Li F, Lu WJ, Yang YZ, Tang XP, Shi ZL (2010a) The research of crisis miners ore-forming regularity and prospecting: on Yunnan Lancang old miners bed for example. Yunnan Science and Technology Press, Kunming (in Chinese)
Li JW, Deng XD, Zhou MF, Liu YS, Zhao XF, Guo JL (2010b) Laser ablation ICP-MS titanite U–Th–Pb dating of hydrothermal ore deposits: a case study of the Tonglushan Cu–Fe–Au skarn deposit, SE Hubei Province, China. Chemical geology 270:56–67
Li XH, Li ZX, Li WX (2014) Detrital zircon U-Pb age and Hf isotope constrains on the generation and reworking of Precambrian continental crust in the Cathaysia Block, South China: a synthesis. Gondwana Research 25:1202–1215
Li G, Deng J, Wang Q, Liang K (2015) Metallogenic model for the Laochang Pb–Zn–Ag–Cu volcanogenic massive sulfide deposit related to a Paleo-Tethys OIB-like volcanic center, SW China. Ore Geology Reviews 70:578–594
Liu Y, Gao S, Hu Z, Gao C, Zong K, Wang D (2010a) Continental and oceanic crust recycling-induced melt-peridotite interactions in the Trans-North China Orogen: U-Pb dating, Hf isotopes and trace elements in zircons from mantle xenoliths. Journal of Petrology 51: 537–571
Liu Y, Hu Z, Zong K, Gao C, Gao S, Xu J, Chen H (2010b) Reappraisement and refinement of zircon U-Pb isotope and trace element analyses by LA-ICP-MS. Chinese Science Bulletin 55: 1535–1546
Long H, Luo T, Chen F, Huang Z, Zhou M, Yang Y, Qian Z (2008) Single grain sphalerite and pyrite Rb-Sr geochronology: implication for timing constraint on Ag-polymetallic Laochang deposit, Lancang, Yunnan. Bulletin of Mineralogy, Petrology and Geochemistry 27: 322–323 (in Chinese with English abstract)
Ludwig KR (2003) ISOPLOT 3.00: a geochronological toolkit for Microsoft Excel. Berkeley Geochronology Center, California, Berkeley.
Mao JW, Ye HS, Wang RT, Dai JZ, Jian W, Xiang JF, Meng F (2009) Mineral deposit model of Mesozoic porphyry Mo and vein-type Pb–Zn–Ag ore deposits in the eastern Qinling, Central China and its implication for prospecting. Geological Bulletin of China 28:72–79 (in Chinese with English abstract)
Mao JW, Pirajno F, Xiang JF, Gao JJ, Ye HS, Li YF, Guo BJ (2011) Mesozoic molybdenum deposits in the east Qinling–Dabie orogenic belt: characteristics and tectonic settings. Ore Geology Reviews 43: 264–293
Mao J, Pirajno F, Lehmann B, Luo M, Berzina A (2014) Distribution of porphyry deposits in the Eurasian continent and their corresponding tectonic settings. Journal of Asian Earth Sciences 79:576–584
Metcalfe I (2006) Palaeozoic and Mesozoic tectonic evolution and palaeogeography of East Asian crustal fragments: the Korean Peninsula in context. Gondwana Research 9:24–46
Metcalfe I (2013) Gondwana dispersion and Asian accretion: tectonic and palaeogeographic evolution of eastern Tethys. Journal of Asian Earth Sciences 66:1–33

Mo XX, Deng JF, Dong FL, Yu XH, Wang Y, Zhou S, Yang WG (2001) Volcanic petrotectonic assemblages in Sanjiang orogenic belt, SW China and implication for tectonics. Geological Journal of China Universities 7:121–138 (in Chinese with English abstract)

Nie X, Feng Q, Qian X, Wang Y (2015) Magmatic record of Prototethyan evolution in SW Yunnan, China: geochemical, zircon U-Pb geochronological and Lu-Hf isotopic evidence from the Huimin metavolcanic rocks in the southern Lancangjiang zone. Gondwana Research 28:757–768

Ouyang C, Xu C (1991) Geochemical features and genesis of the Laochang Diwa-type silver-lead ore deposit in Langchang, Yunnan, China. Geotectonica et Metallogenia 15:317–326 (in Chinese with English abstract)

Plumlee GS, Montour M, Taylor CD, Wallace AR, Klein DP (1995) Polymetallic vein and replacement deposits. Preliminary compilation of descriptive geoenvironmental mineral deposit models US Geological Survey Open-File Report: 95–831

Qi L, Gao J, Zhou M, Hu J (2013) The design of re-usable carius tubes for the determination of rhenium, osmium and platinum-group elements in geological samples. Geostandards and Geoanalytical Research 37:345–351

Qi L, Zhou MF, Gao J, Zhao Z (2010) An improved Carius tube technique for determination of low concentrations of Re and Os in pyrites. Journal of Analytical Atomic Spectrometry 25:585–589

Shirey SB, Walker RJ (1998) The Re-Os isotope system in cosmochemistry and high-temperature geochemistry. Annual Review of Earth and Planetary Sciences 26:423–500

Sillitoe RH (2010) Porphyry copper systems. Economic Geology 105:3–41

Simmons SF, White NC, John DA (2005) Geological characteristics of epithermal precious and base metal deposits. Economic Geology 100th Anniversary Volume: 485–522.

Titley SR (1993) Characteristics of porphyry copper occurrence in the American Southwest. Mineral Deposit Modelling: Geologic Association of Canada, Special Paper 40:433–464

Wang B, Wang L, Pan G, Yin F, Wang D, Tang Y (2013) U-Pb zircon dating of Early Paleozoic gabbro from the Nantinghe ophiolite in the Changning-Menglian suture zone and its geological implication. Chinese Science Bulletin 58:920–930

Wang D, Qu W, Li Z, Yin H, Chen Y (2005) Mineralization episode of porphyry copper deposits in the Jinshajiang-Red River mineralization belt: Re-Os dating. Science in China Series D: Earth Sciences 48:192–198

Wang R (2007) Liner-ring structure of remote sensing studies: implication for ore exploration in Laochang, Lancang area. Kunming University of Science and Technology, Yunnan (in Chinese)

Wiedenbeck M, Alle P, Corfu F, Griffin WL, Meier M, Oberli F, QuadtAv, RoddickJC, SpiegelW (1995) Three natural zircon standards for U-Th-Pb, Lu-Hf, trace element and REE analyses. Geostand Newslett 19:1–23

Xu C, Ouyang C (1991) A study on the genesis of the Ag-Pb-Zn deposit in Laochang, Lancang, Yunnan. Journal of Guilin College of Geology 11:245–252 (in Chinese with English abstract)

Xue B (1989) The discussion of the gensis of Laochang Pb-Zn deposit in Lancang. Yunnan Geology 8:181–188 (in Chinese with English abstract)

Yang F, Li F, Chen H, Xiao J, Zhao X (2012) Geochemistry and tectonic setting of the Laochang concealed granite porphyry in Lancang, Yunnan Province. Acta Petrologica Et Mineralogica 31:39–49 (in Chinese with English abstract)

Yang K, Mo X (1993) Characteristics of the Laochang volcanic massive sulfide deposit, southwestern Yunnan, China. Exploration and Mining Geology 2:31–40

Yang K, Scott SD, Mo X (1999) Massive sulfide deposits in the Changning-Menglian back-arc belt in western Yunnan, China; comparison with modern analogues in the Pacific. Exploration and Mining Geology 8:211–231

Yang TN, Ding Y, Zhang HR, Fan JW, Liang MJ, Wang XH (2014) Two-phase subduction and subsequent collision defines the Paleotethyan tectonics of the southeastern Tibetan Plateau: evidence from zircon U-Pb dating, geochemistry, and structural geology of the Sanjiang orogenic belt, southwest China. Geological Society of America Bulletin 126:1654–1682

YBGMR-Yunnan Bureau of Geology and Mineral Resources (1990) Regional geology of Yunnan Province. Geological Memoir Series, 1 (21). Beijing, Geological Publishing House (in Chinese).

Zhai MG, Cong BL, Qiao GS, Zhang RY (1990) Sm-Nd and Rb-Sr geochronology of metamorphic rocks from SW Yunnan orogenic zones, China. Acta Petrologica Sinica 4:1–11 (in Chinese with English abstract)

Zhang R, Cong B, Maruyama S, Liou JG (1993) Metamorphism and tectonic evolution of the Lancang paired metamorphic belts, southwestern China. Journal of Metamorphic Geology 11:605–619

Zhang Y, Duan J (2001) Study on tectonic evolution of ophilite and Lancangjiang plate suture in West Yunnan. Kuming, Yunnan Science and Technology Press (in Chinese).

Zeng PS, Hou ZQ, Gao YF, Du AD (2006) The Himalayan Cu-Mo-Au mineralization in the eastern Indo-Asian collision zone: constraints from Re-Os dating of molybdenite. Geological Review 52:72–84 (in Chinese with English abstract)

Zhong DL (1998) The Paleotethys orogenic belt in west of Sichuan and Yunnan: Beijing, Science Publishing House (in Chinese).

Zhong H, Hu R, Ye Z, Tu G (2000) Isotope geochronology of Dapingzhang spilite-keratophyre formation in Yunnan Province and its geological significance. Science in China Series D: Earth Sciences 43:200–207

Zhou MF, Yan DP, KennedyAK LY, Ding J (2002) SHRIMP U-Pb zircon geochronological and geochemical evidence for Neoproterozoic arc-magmatism along the western margin of the Yangtze Block, South China. Earth and Planetary Science Letters 196:51–67

Zhou MF, Zhao XF, Chen WT, Li XC, Wang W, Yan DP, Qiu HN (2014) Proterozoic Fe-Cu metallogeny and supercontinental cycles of the southwestern Yangtze Block, southern China and northern Vietnam. Earth-Science Reviews 139:59–82